

Production of Characteristic X-Rays by Protons of 1.7- to 3-Mev Energy*

H. W. LEWIS AND B. E. SIMMONS,† *Duke University, Durham, North Carolina*

AND

E. MERZBACHER, *University of North Carolina, Chapel Hill, North Carolina*

(Received February 24, 1953)

Characteristic x-rays produced when protons of 1.7- to 3-Mev energy are stopped in thick targets of Mo, Ag, Ta, Au, and Pb have been studied using a NaI scintillator. *K* and *L* radiation for the three heavy elements produced well-separated differential pulse-height peaks, while only the *K* radiation was detectable for Mo and Ag. Cross sections for *K* ionization have been calculated, with corrections for the Auger effect, and compared with the theory. Ratios of experimental to theoretical cross sections vary from one to four, with good agreement for the light elements and low proton energies. The measured cross sections at 2.4-Mev proton energy are 11, 3.0, 0.036, 0.016, and 0.010 barns for Mo, Ag, Ta, Au, and Pb, respectively.

I. INTRODUCTION

THE ionization of an atom through removal of an electron from an inner shell by the impact of a heavy particle (proton, deuteron, alpha particle) and the subsequent emission of an x-ray has received sporadic attention since Chadwick and others in 1913 first observed and identified the characteristic x-rays of several elements exposed to alpha rays. A thorough investigation of inner shell ionization in various elements by alpha particles from a polonium source was published in 1928 by Bothe and Fränz¹ where references to the older work are also found. They used a Geiger counter to measure excitation functions up to an energy of 5.1 Mev. *K*-, *L*-, and *M*-shell x-rays were observed from elements with $Z=12$ to 30, $Z=34$ to 79, and $Z=83$, respectively. An absolute cross-section measurement, using an ionization chamber, was made only for the *K* radiation from aluminum. Since this method was not sensitive enough to be applied to the considerably weaker x-ray intensities from elements of higher Z , all the other cross-section values in Bothe's paper are only estimates which lead to the qualitative conclusion that the probability of x-ray excitation falls rapidly with increasing Z . For each element the cross section was shown to increase approximately as the 4.5th power of the incident energy. Comparing pairs of elements whose *K*- and *L*-absorption edges were about the same they found the x-ray intensities of the member of each pair to be approximately equal.

Cork² in 1941 used deuterons with energies up to 10 Mev and examined the blackening of photographic plates by x-rays from thirty-eight elements. While the qualitative features of Bothe's conclusions were reproduced, i.e., increase of cross section with increasing energy and decreasing atomic number, no accurate quantitative results were presented.

With protons as the incident particles the first successful experiments were performed by Gerthsen and

Reusse³ after Barton⁴ had vainly searched for x-rays produced by low energy protons. They used protons with energies between 30 and 150 kev and, with a Geiger counter, observed the *K* radiation from Al and Mg as well as *L* radiation from Se. Excitation functions were measured, and an absolute cross-section measurement for the *K* radiation from Al with an incident proton energy of 132 kev was later added by Peter.⁵ Qualitatively, the results were the same as those of Bothe and Fränz.

Livingston, Genevese, and Konopinski⁶ finally used protons up to 1.72 Mev. With an ionization chamber they measured the intensity as a function of Z ($Z=12$ to 42 for *K*-, $Z=42$ to 82 for *L* radiation) and estimated the order of magnitude of the cross sections.

Related to the phenomenon under discussion here is the *K*-shell ionization accompanying the decay of α emitters such as Po²¹⁰, where the α particle ionizes directly the atom from which it has been emitted. Most recently Barber and Helm⁷ have investigated this effect for which theoretical probabilities were worked out by Migdal.⁸

In the present experiments the use of a NaI scintillation counter as a detector of x-rays permits the study of the *K* radiations from elements above $Z=42$ and of the *L* radiations from several of the highest Z elements—all hard enough to be detected by the crystal, and, in the case of *K* radiation, too weak in intensity to have been measured by previous workers.

Theoretical predictions for the cross sections to be expected for the *K*-shell ionization by slow protons and alpha particles were made by Henneberg⁹ in 1933. While all previously reported cross sections were, within the rather large experimental uncertainties, in agreement with Henneberg's nonrelativistic theory, the present data indicate deviations from the calculated cross

³ C. Gerthsen and W. Reusse, *Physik Z.* **34**, 478 (1933).

⁴ H. A. Barton, *J. Franklin Inst.* **209**, 1 (1930).

⁵ Otto von Peter, *Ann. Physik* **27**, 299 (1936).

⁶ Livingston, Genevese, Konopinski, *Phys. Rev.* **51**, 835 (1937).

⁷ W. Barber and R. Helm, *Phys. Rev.* **86**, 275 (1952).

⁸ A. Migdal, *J. phys. (U.S.S.R.)* **4**, 449 (1941).

⁹ W. Henneberg, *Z. Physik* **86**, 592 (1933).

* Supported by the U. S. Atomic Energy Commission.

† Now at the University of Minnesota, Minneapolis, Minnesota.

¹ W. Bothe and H. Fränz, *Z. Physik* **52**, 466 (1928).

² J. M. Cork, *Phys. Rev.* **59**, 957 (1941).

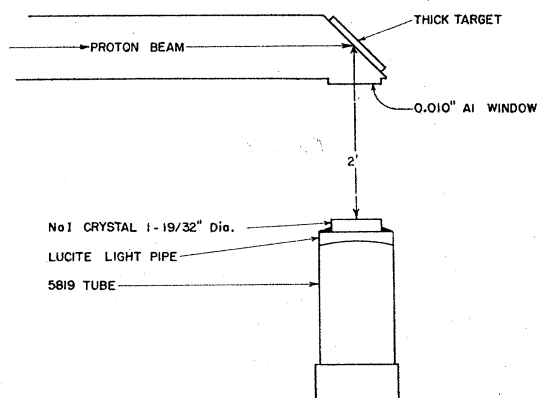


FIG. 1. Arrangement of target and scintillation detector.

sections, particularly for high atomic numbers. Although we have measured several cases of *L*-shell ionization, the corrections attributable to absorption are very large so that more refined measurements are needed in order to obtain reliable values of cross sections. Furthermore there are no published theoretical calculations.

II. EXPERIMENTAL ARRANGEMENT

Figure 1 shows the arrangement of target and detector. The former was placed at an angle of 45° to the proton beam from the Van de Graaff accelerator and consisted of a flat plate held against an O-ring seal by atmospheric pressure. The x-radiation produced in the target passed through the 0.010-in. aluminum side

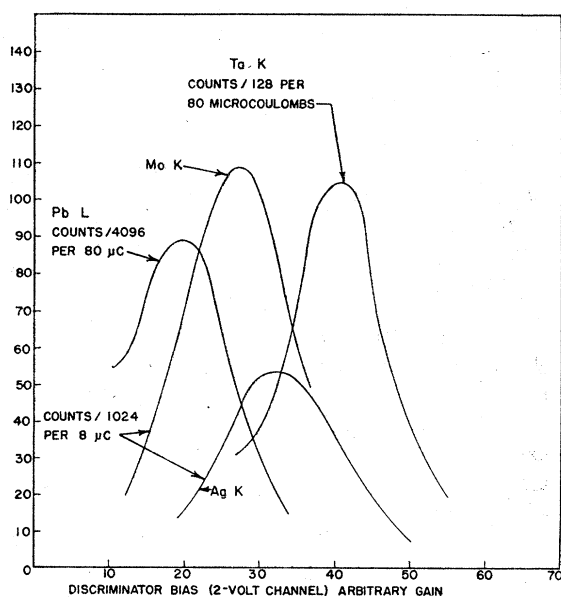


FIG. 2. Thick target counting rates vs discriminating bias at proton energy 2.40 Mev. Rates are uncorrected for target and Al-air absorption. Scaler setting and current integrator charge are designated on each curve.

window to the NaI scintillator two feet from the target. This crystal, of diameter $1\frac{19}{32}$ in. and thickness $\frac{1}{2}$ in., was manufactured and canned by the Harshaw Chemical Company. The aluminum can walls were 0.025 in. thick. A Lucite light pipe $\frac{1}{2}$ in. long coupled the crystal to the 5819 phototube.

Pulses from the phototube were fed through a cathode follower preamplifier, A-1 linear amplifier, and single-channel differential pulse-height selector to a scaler. The current integrator for the proton beam consisted of a 0.002- μ f condenser connected across an OB2 gas tube, which activated the scaler when the tube fired. This integrator was calibrated artificially by a constant current source for a known time, yielding a calibration of 0.100 ± 0.003 microcoulombs per scaler count. Some of the later data were taken with a more elegant elec-

TABLE I. Yields of *K*-shell x-rays from protons of energy *E*.

1	2	3	4	5	6	7
Element	Z	<i>E</i> in keV	<i>E</i> in MeV	<i>J</i>	<i>C</i>	<i>I</i> _μ
Mo	42	20.0	2.40	1.2×10^7	3.7	3.2×10^{-4}
Ag	47	25.5	1.70	0.11×10^7	2.1	0.17×10^{-4}
			1.92	0.22	0.33	
			2.17	0.37	0.56	
			2.40	0.56	0.86	
			2.64	0.87	1.3	
Ta	73	67.4	1.92	0.44×10^8	1.08	3.4×10^{-7}
			2.17	0.80	6.2	
			2.40	1.2	9.4	
			2.64	2.24	18	
			2.88	3.08	24	
Au	79	80.5	2.40	5.3×10^4	1.07	4.1×10^{-7}
			2.17	1.8	1.4	
			2.40	3.3	2.6	
			2.88	11	8.5	
Pb	82	87.6	1.92	1.0×10^4	1.07	0.80×10^{-7}
			2.17	1.8	1.4	
			2.40	3.3	2.6	
			2.88	11	8.5	

tronic integrator, with consistent results. In some cases scintillator counting rates were so high, even with beam currents well below one microampere, that considerable care had to be taken to avoid pileup of pulses in the associated circuits.

Differential pulse-height distributions were measured for Mo, Ag, Ta, Au, and Pb. Photons of energy below about 10 keV gave pulses near tube noise and hence only those x-ray series with energies greater than this value were measured. Both *K* and *L* series were measurable for the three heavy elements and only the *K* series for Mo and Ag. Lines in a given series cannot, of course, be resolved. A differential pulse-height peak for a given series is obtained whose width is due partly to the presence of several lines of different energies in a series and partly to crystal and phototube resolution. Typical counting rate peaks taken with a 2-volt channel width are shown in Fig. 2.

III. EXPERIMENTAL RESULTS

To obtain the total number of x-rays produced in the target, the following calculations must be made:

(a) Find the integrated number of counts under the counting rate peak. The number J of light quanta counted per $N=5 \times 10^{14}$ incident protons is listed in column 5 of Table I.

(b) Apply the solid angle correction for the $1\frac{1}{3}\frac{9}{2}$ -in. diameter scintillator at a distance of two feet from the target.

(c) Correct for the absorption of x radiation in the target chamber window (0.010-in. Al), two feet of air, and the crystal housing (0.025-in. Al). C in column 6 of Table I is the over-all correction factor.

(d) Correct for the self-absorption in the target in the case of thick targets. The thick target results were supplemented by and found consistent with some thin target measurements on Ag and Au.

The number of light quanta emitted from a thick target into a solid angle Ω per N incident protons of energy E and range x_0 is given by

$$CJ = \frac{\Omega}{4\pi} N n \rho \int_0^{x_0} e^{-\mu(x_0-x)} \sigma[E(x)] dx, \quad (1)$$

where $\sigma[E(x)]$ denotes the cross section for ionization with K -shell x-ray emission. μ is the average absorption coefficient of the target for its own characteristic x-radiation, n denotes the number of target atoms per gram, and ρ is the density of the target.

The values of the quantity

$$I_\mu(x_0) = \frac{4\pi CJ}{\Omega N} = n \rho \int_0^{x_0} e^{-\mu(x_0-x)} \sigma[E(x)] dx \quad (2)$$

are listed in column 7 of Table I. Evidently

$$I_0(x_0) = n \rho \int_0^{x_0} \sigma[E(x)] dx \quad (3)$$

is the number of K -shell light quanta emitted when a proton is stopped in the target.

Proceeding like Bothe and Fränzl, we obtain by differentiation of Eq. (2)

$$\sigma[E(x)] = \frac{1}{n\rho} \frac{dI_\mu(x)}{dx} + \frac{\mu}{n\rho} I_\mu(x) = -\frac{1}{n} \frac{dI_\mu(x)}{dE} \frac{dE}{d(\rho x)} + \frac{\mu}{n\rho} I_\mu(x). \quad (4)$$

Substitution of this expression in Eq. (3) leads to

$$I_0(x_0) = I_\mu(x_0) + \mu \int_0^{x_0} I_\mu(x) dx. \quad (5)$$

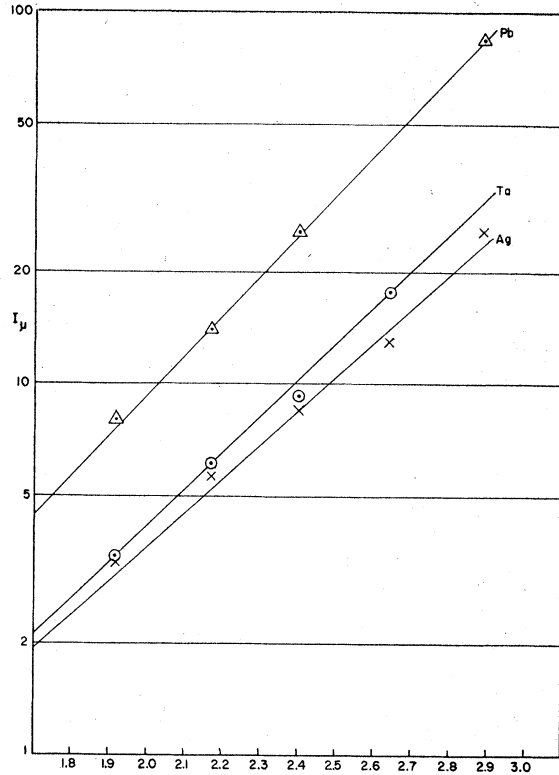


FIG. 3. I_μ of Eq. (2) as a function of proton energy in Mev for thick targets of Ag, Ta, and Pb.

Since the cross section rather than the yield I_0 is of primary interest, we did not compute the latter here. I_μ as a function of energy has been plotted in Fig. 3 for Ag, Au, and Pb. The derivative of I_μ was determined graphically from these plots. Column 3 of Table II contains the cross sections evaluated from Eq. (4). The following computed average mass-absorption

TABLE II. Experimental and theoretical cross sections (in cm^2).

Element	2	3	4	5	6	7
	E	σ	Auger factor	σ_K	σ_{th}	Φ
Mo	2.40	8.0×10^{-24}	1.4	11×10^{-24}	6.60×10^{-24}	0.0794
Ag	1.70	0.53×10^{-24}	1.3	0.69×10^{-24}	0.756×10^{-24}	0.00771
	1.92	1.0		1.3	1.15	0.0145
	2.17	1.6		2.1	1.61	0.0234
	2.40	2.3		3.0	2.20	0.0335
	2.64	3.3		4.3	2.77	0.0481
	2.88	6.3		8.2	3.49	0.0916
Ta	1.92	13×10^{-27}	1.1	14×10^{-27}	6.44×10^{-27}	0.000956
	2.17	23		25	9.73	0.00171
	2.40	33		36	14.0	0.00246
	2.64	60		66	18.8	0.00452
	2.88	77		85	26.3	0.00581
	3.15	110		120	34.8	0.00820
Au	2.40	16×10^{-27}	1.0	16×10^{-27}	5.56×10^{-27}	0.00150
Pb	1.92	3.6×10^{-27}	1.0	3.6×10^{-27}	1.56×10^{-27}	0.000391
	2.17	5.9		5.9	2.48	0.000641
	2.40	10.5		10.5	3.43	0.00114
	2.88	30.5		30.5	6.30	0.00331

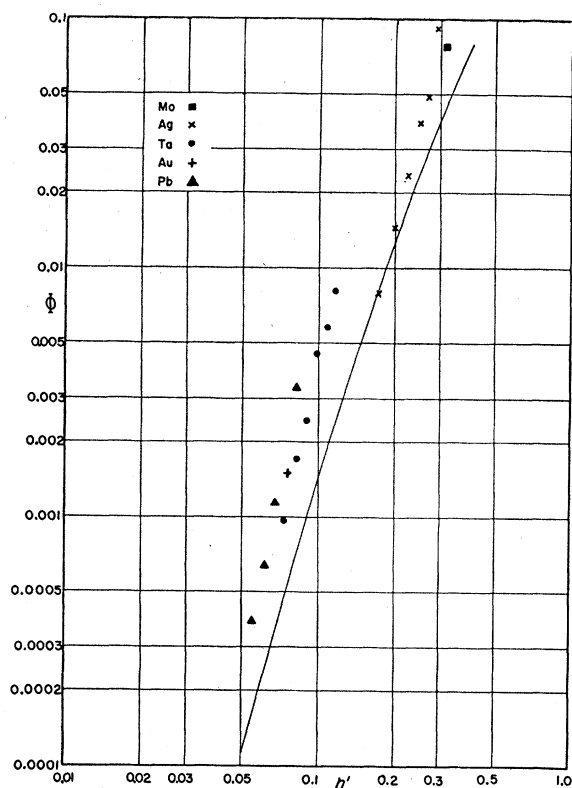


FIG. 4. Comparison of experimental results with theoretical predictions. η' is defined in Eq. (7). The solid curve represents the theoretical function Φ_0 (see text); the experimental points are related to the cross sections by Eq. (8).

coefficients were employed:

Element	Mo	Ag	Ta	Au	Pb
Av. mass-abs. coeff. (cm ² /g)	18.3	13.5	3.38	2.61	2.27

The very nearly exponential dependence of I_μ on E , within the proton energy range used, as seen in Fig. 3, was made the basis of an interpolation for the other elements. For the values of energy loss the calculations of Aron¹⁰ were used.

Comparison with the theory is only possible after radiationless (Auger) transitions have been taken into account. Estimated correction factors were taken from Massey and Burhop.¹¹ σ_K in column 5 of Table II is the total cross section for K -shell ionization.

¹⁰ W. A. Aron, University of California Radiation Laboratory Report-1325, 1951 (unpublished).

¹¹ H. S. W. Massey and E. H. S. Burhop, Proc. Roy. Soc. (London) A153, 661 (1936).

IV. COMPARISON WITH THE THEORY

Henneberg,⁹ having justified the use of the Born approximation in the analysis of K -shell ionization by slow heavy particles, obtained from Bethe's general nonrelativistic theory an approximate formula for the cross section:

$$\sigma_{th} = \frac{3.51}{Z^4\theta} \Phi_0(\eta') \times 10^{-16} \text{ cm}^2. \quad (6)$$

θ is the ratio of the observed K -shell ionization energy E_K to the "ideal ionization energy in the absence of outer screening," and Φ_0 a dimensionless function defined by Henneberg, Eq. (13), and plotted as the solid curve in Fig. 4. The quantity η' is given as

$$\eta' = 4mE/M\theta E_K, \quad (7)$$

M/m being the ratio of the mass of the heavy incident particle to the mass of the electron.

Column 6 of Table II lists the theoretical cross sections; column 7 gives the experimental quantity

$$\Phi = (Z^4\theta/3.51) \times \sigma_K \times 10^{16}, \quad (8)$$

and the corresponding points appear on Fig. 4. The values of θ used here were 0.82 for Mo and Ag, and 0.86 for Ta, Au, and Pb, as computed from the relativistic "ideal" ionization energies,¹² although the use of relativistic values for the screening factor is a somewhat inconsistent procedure. Nonrelativistic values of θ (0.85 for the two lighter and 0.95 for the three heavier elements) lead to theoretical cross sections smaller by ten to fifty percent than those listed in Table II.

The largest source of error in the experiment is in determining the value of J itself and we estimate this error to be not greater than 25 percent. It is evident from Table II and Fig. 4 that, while there is general agreement between experiment and theory, the latter predicts cross sections which are low, particularly for the heavy elements and for higher proton energies even when the smaller values for θ are adopted. The fact that the discrepancy is greater for high atomic numbers than for low ones and the improvement due to relativistic values for θ suggest that a consistent relativistic treatment of the K electrons might bring theory and experiment into closer agreement.

¹² We are indebted to H. Bethe and C. Walske for valuable comments.